Performance of Spatial Division Multiplexing MIMO with Frequency Domain Packet Scheduling

From Theory to Practice

Wei, Na; Pokhariyal, Akhilesh; Sørensen, Troels Bundgaard; Kolding, Troels E.; Mogensen, Preben

Published in:
IEEE Journal on Selected Areas in Communications

DOI (link to publication from Publisher):
10.1109/JSAC.2008.080806

Publication date:
2008

Document Version
Accepted author manuscript, peer reviewed version

Performance of Spatial Division Multiplexing MIMO with Frequency Domain Packet Scheduling: From Theory to Practice

Na Wei[(1)], Akhilesh Pokhariyal[(1)],
Troels B. Sørensen[(1)], Troels E. Kolding[(2)], Preben E. Mogensen[(1,2)]
[(1)]Department of Electronic Systems, Aalborg University,
Fredrik Bajers Vej 7, Aalborg, Denmark.
[(2)]Nokia Siemens Networks, Niels Jernes Vej 10, Aalborg, Denmark.

Abstract

This paper addresses the performance of Spatial Division Multiplexing (SDM) Multiple-input Multiple-output (MIMO) techniques together with Frequency Domain Packet Scheduling (FDPS) in both theory and practice. We start with a theoretical analysis under some ideal assumptions to derive the performance bounds of SDM-FDPS. To facilitate the analysis, a unified SINR concept is utilized to make a fair comparison of MIMO schemes with different number of spatial streams. The effect of packet scheduling is included in the post-scheduling SINR distribution using an analytical model. Based on that, the performance bounds are obtained with a more realistic SINR to throughput mapping metric. The system-level performance of SDM-FDPS has been evaluated under practical constraints using detailed simulations based on the UTRAN Long Term Evolution (LTE) downlink cellular system framework. The purpose is to investigate the impact of realistic factors on performance. Results confirm that the combination of SDM and FDPS can increase the spectral efficiency significantly, particularly in a micro-cell scenario, and up to 30%-60% gain is observed over 1x2 with FDPS depending on the traffic models considered. Finally, the more practical simulation results are compared against the theoretical performance bounds. A performance loss is seen in the simulations due to realistic coding/modulation, impact of frequency selectivity, signalling constraints, imperfect channel quality indicator (CQI), etc.

Index Terms

Frequency Domain Packet Scheduling, Opportunistic Scheduling, Spatial Division Multiplexing MIMO, Performance Bound, System-level Performance, UTRAN Long Term Evolution.

I. Introduction

A. Prior Work and Motivation

WHEN multiple users are present in the 3G or its enhancement systems, channel aware opportunistic packet scheduling can be employed to boost the spectral efficiency, by exploiting the multi-user diversity gain in the time domain [1]. Orthogonal Frequency Domain Multiplexing (OFDM) has gradually become the dominant air interface for most next generation wireless systems, such as Digital Audio Broadcasting (DAB) [2], Digital Video Broadcasting (DVB-T) [3], the IEEE 802.11 local area network (LAN) standard [4], the IEEE 802.16 metropolitan area network (MAN) standard [5] and UTRA Long Term Evolution (LTE) [6]. One of the advantages of OFDM(A) is that the multi-user concept can be extended to the frequency domain. As the name suggests OFDMA is a multi-user version of the OFDM digital modulation scheme. The packet scheduling concept in OFDMA is termed as Frequency Domain Packet Scheduling (FDPS), and it can bring a significant gain to the system, by exploiting the multiuser

This work has appeared in part in the 65th IEEE Proc. Vehicular Technology Conf., Dublin, Ireland, Apr. 2007. The contact email: {tbs,pm}@es.aau.dk.

diversity in both time and frequency domains. Optimal and sub-optimal sub-carrier based adaptation has been widely studied in the literature, see [7] [8] and the references therein. The concept is studied with more realistic assumptions using the UTRA LTE framework in our earlier work [9] where subband adaptation and channel quality indication (CQI) issues are included. These studies have shown that FDPS can achieve up to 40%-60% cell throughput gain over time-domain only scheduling, based on the 1x2 antenna scheme and the MRC receiver [9].

The Multiple-input Multiple-output (MIMO) in Spatial Division Multiplexing (SDM) mode can also provide a large spectral efficiency gain without increasing power or bandwidth. Considering a general multiuser MIMO system, the sum-rate capacity of MIMO broadcast channels was analyzed in [10]. The dirty paper algorithm [11] is identified as the best strategy to achieve that. Unfortunately, the high complexity of this algorithm and its prerequisite of perfect information of all the users' channel information at the transmitter makes it difficult for practical implementation. The problem is addressed with much less complex linear receivers by Heath in [12] where some sub-optimal solutions have been proposed.

Considering the potentials from SDM and FDPS, it is therefore quite natural to consider the combination of them (SDM-FDPS) to exploit the multi-user gain in space, frequency and time. To achieve the optimality for SDM-FDPS, the bit and power loading issues of FDPS have to be jointed optimized with MIMO selection, which results in quite high complexity and extremely high signalling requirements for frequency-division duplex (FDD) mode systems (see for example the exhaustive search algorithm in [13]). The studies in in [14] [15] [16] addressed the multiple dimension problem from an information theory point of view, which provides very good insight in the performance bounds.

In terms of practical SDM-FDPS schemes, two schemes are considered for UTRA LTE in 3GPP [6]. They are referred to as Single-User (SU-) and Multi-User (MU-) MIMO. The SU-MIMO has the restriction that only one User Equipment (UE) can be scheduled over the same time-frequency resource across all spatial streams, whereas MU-MIMO offers greater flexibility to the scheduler so that different UEs can be scheduled on different spatial streams over the same time-frequency resource. The MU-MIMO offers greater flexibility in the spatial domain, but it also imposes higher requirements on the resource allocation signalling. Moreover, both schemes should be based on subband adaptation, and the evaluation should include signalling constraints and some realistic issues from practical system.

Most previous theoretical studies consider only ideal SDM-FDPS schemes under rather ideal assumptions, which makes the performance bounds too optimistic. For example, most studies use only the ideal Shannon capacity as a performance metric. As shown in [17], the ideal Shannon formula gives very optimistic performance compared to realistic link adaptation with realistic modulation and coding. Besides, most previous studies ignore the analysis of SU-MIMO due to its sub-optimality and mathematic difficulty. However, the SU-MIMO is quite crucial for practical implementation due to its much reduced complexity and less signalling overhead. Besides, the SU-MIMO is able to support advanced interference cancellation receiver to improve performance [18], but MU-MIMO can not do that [19]. The tradeoff of complexity, signalling and performance gain of SU- and MU- MIMO should be analyzed to identify better compromise solution for practical system. Therefore, we set it as a goal to derive **tight** performance bounds based on realistic system-level assumptions for both SU-MIMO and MU-MIMO cases.

Although the theoretical analysis under ideal assumptions is useful to gain insight on upper bounds, it has limitations as it does not include the impact of many realistic factors such as fairness between UEs, frequency selectivity within a frequency band, limited dynamic range of SINR in the cell, traffic variations, the amount of signaling overhead, adaptation uncertainties, etc. Such factors are highly relevant in wireless system design and need to be addressed as well. This necessitates the system-level simulation study which is considered as the second target for this study. However before we can proceed on to the system level analysis, practical scheduling algorithms with signalling overhead constraints need to be designed taking into account the interaction of SDM schemes with other functional entities in the system already such as Link Adaptation (LA) and Hybrid ARQ (HARQ).

B. Contribution

The main contribution of this paper is the performance analysis of SDM MIMO combined with FDPS from both a theoretical as well as a system-level simulation standpoint. Both approaches are required to gain a better understanding of the gain mechanisms of SDM-FDPS, and to investigate the impact of practical system aspects on the achievable performance.

To derive the theoretical bounds, we start with an analysis on the distribution of post-scheduling SINR for the combination of SDM and Proportional Fair (PF) FDPS. The simplified analytical PF model in [20] has been utilized. To facilitate the analysis, a unified SINR concept is proposed in which all multi-stream MIMO SINRs are translated into an equivalent effective SINR offering the same total capacity. The distribution analysis gives a good insight into the interrelation between SDM MIMO and PF scheduling algorithms and provides important hints on the algorithm design. Further, the modified Shannon capacity formula in [17] is adopted here as the performance metric since it can better describe the practical link adaptation performance. All these considerations not only make the SU-MIMO analysis feasible but are also shown to be very effective on tightening the performance bounds for both SU- and MU- MIMO schemes.

The drawback of the theoretical analysis is that it is difficult to include the impact from many practical issues such as signalling constraints, fairness between users, frequency selectivity, band adaptation, imperfect CQI, etc. Therefore, system level simulations are performed as well to evaluate more realistic achievable gain of SDM-FDPS. As a case study, we will focus on the downlink of a UTRA LTE FDD system [6]. All the essential gain mechanisms for LTE such as LA, HARQ L1 retransmission and combining, packet scheduling, etc are included. Although the LTE is selected as the case study here, the analysis is general applicable for most other MIMO-OFDM systems such as WiMAX. Before the evaluation can be performed, practical scheduling algorithm are designed for SU-MIMO and MU-MIMO by taking many practical issues into account. For example, since SDM schemes can only be applied on the time-frequency resources experiencing favorable channel conditions, transmit diversity schemes should be used as the fall back MIMO mode. The link adaptation therefore also involves MIMO adaptation. Moreover, due to the signalling overhead concerns we impose constraints on the FDPS algorithm such that only one MIMO mode is allowed for one UE within one Transmission Time Interval (TTI), which will make the performance suboptimum. The proposed scheduling algorithm design is efficient and suitable for practical implementation. The network performance evaluation reveals also the impact from different cellular deployment scenarios, precoding effect, traffic models, etc.

Finally, the practical performance of SDM-FDPS is compared against the theoretical bounds. The loss in performance from real simulations compared to the performance bounds is due to the issues such as frequency selectivity within a frequency chunk, signalling constraints, CQI imperfections, etc.

C. Organization

The paper is organized as follows. The SDM-FDPS system model under the framework of UTRA LTE downlink is outlined in Section II. The theoretical analysis of performance bounds is conducted in Section III with some simplified assumptions. The system level simulation results are presented and analyzed in Section IV. The performance from the theory and simulation is compared in V. Finally, the concluding remarks are provided in Section VI.

II. SDM-FDPS System Model

Consider a UTRA LTE FDD mode downlink consisting of a scheduling node (eNode-B) with FDPS functionality and several UEs with SDM capability. All UEs measure the channel quality at every TTI, and the measurement is formatted as a CQI report and forwarded to the eNode-B in the uplink. Based on the CQI reports the eNode-B performs fast channel aware packet scheduling in the space-frequency-time domains as well as data rate adaptation, as shown in Fig. 1. In addition to the traditional beamforming and/or diversity MIMO FDPS [9], the SU-MIMO and MU-MIMO cases are also considered for LTE [19].

Diversity MIMO is referred to space-time block code family which are maximized to improve diversity only. The basic scheduling unit is denoted as the Physical Resource Block (PRB). As stated in [6] for diversity MIMO and SU-MIMO, the minimal scheduling resolution is one PRB (over all the streams), which covers a group of 25 neighboring sub-carriers corresponding to around 375kHz bandwidth, over 7 OFDM symbols [1]. However, the PRB is defined on a single spatial stream incase of MU-MIMO. The Fig. 2 illustrates the definition of PRB for the two SDM-FDPS concepts under investigation, considering a maximum of two spatial streams. Note that SU-MIMO is a special case of MU-MIMO, i.e., when the same UE gets allocated the same time-frequency resource on all streams. The allocation of PRBs to UEs is determined by the eNode-B scheduler, together with the Modulation and Coding Set (MCS) for these resources. The scheduler interacts with entities such as LA and the HARQ manager during the execution of the scheduling algorithm.

As a basis for this study we consider the well-known PF algorithm which provides an attractive trade-off between throughput and coverage gain [21]. Here we extend the PF algorithm to the spatial domain for MU-MIMO. We estimate the equivalent and instantaneously supported throughput $R_{k,b,s}(t)$ for each UE k, on each frequency chunk b and for each stream s in the scheduling interval t. The PF scheduler selects the k^*th UE on each PRB which maximizes the PF metric $\frac{R_{k,b,s}(t)}{T_k(t)}$,

$$k^* \quad = \quad \arg\max_k \left\{ \frac{R_{k,b,s}(t)}{T_k(t)} \right\}, \quad k = 1...K, \quad \forall b, s \tag{1}$$

where $T_k(t)$ is the average delivered throughput to UE k in the past, which could be calculated by an autoregressive filter [22]. Note that for SU-MIMO and diversity MIMO, since the size of a PRB covers both streams on the same frequency chunk, we still use Eqn. (1), but without the spatial domain flexibility.

III. Theoretical Analysis

The theoretical bounds of the SDM-FDPS performance are derived in this section for both SU-MIMO and MU-MIMO. It is a two step procedure, first the post-scheduling SINR distribution is analysed in subsection III-A. In the final step, we calculate the cell throughput bounds using the SINR to throughput mapping metrics, as described in subsection III-B.

A. Distribution of Post-Scheduling SINR

In this section, in order to gain insight into MIMO-FDPS principles, especially for SDM-FDPS, we consider the post-scheduling SINR distribution using a simple analytical model for the PF scheduler, which was originally used for the SISO antenna scheme with time domain scheduling in [20]. To simplify the analysis, we assume that the frequency chunk bandwidth is smaller than the coherence bandwidth of the channel, and the per frequency chunk fading characteristics are equivalent to the flat-fading Rayleigh channel statistics, then the FDPS in a frequency selective channel is equivalent to time domain Packet Scheduler in flat Rayleigh channel. Besides, as in [20] other simplifying assumptions are adopted to enable the development of a simple analytical model:

1) The fading statistics of all users are independent and identically distributed (i.i.d.). Users move with the same speed and have equal access probability.
2) A user's achievable data rate is (approximately) linearly related to its instantaneous received SINR.
3) A sufficiently long averaging window is used, so that the average received data rate of a user is stationary. On the other hand, the window size is still realistic such that the PF property will not be changed.

[1]The parameter assumptions are following the LTE study item assumptions. In the work item phase, the PRB size is changed to smaller size. However, the results are quite similar since the new parameters updates are more meant for VoIP services, and will not impact significantly on the data service.

While these assumptions are unlikely to be perfectly fulfilled in reality, they suffice to provide insight into the PF scheduler and simplify the PF model. Based on these arguments and assumptions, we can directly adopt the model from [20] where the PF metric in Eqn. (1) can be approximated by

$$k^* = \arg\max_k(\frac{\gamma_k(t)}{\overline{\gamma_k}}), \quad k = 1...K \quad , \tag{2}$$

where $\gamma_k(t)$ is the instantaneous SINR for the kth user at scheduling interval t, and $\overline{\gamma_k}$ is the average received SINR for the kth user. Let the *cumulative distribution function* (CDF) of the SINR for the kth user be $F_{\gamma_k}(\gamma)$. With K active users available for scheduling, denoted as user diversity order, the CDF of the normalized post-scheduling SINR γ^* is given by [23]

$$F_{\gamma^*}(\gamma) = (F_{\gamma_k}(\frac{\gamma_k}{\overline{\gamma_k}}))^K \quad . \tag{3}$$

In case of spatial multiplexing scheme for one user with equal power allocation, the *probability density function* (PDF) of SINR on s^{th} stream γ_s, assuming N_t transmit antennas and N_r receive antennas in flat Rayleigh channels, is given by [24] [25]:

$$p(\gamma_s) = \frac{N_t e^{-\frac{N_t\gamma_s}{\gamma_0}}}{\gamma_0(N_r - N_t)!}(\frac{N_t\gamma_s}{\gamma_0})^{N_r - N_t}, \quad N_r \geq N_t \quad . \tag{4}$$

where the γ_0 is the averaged SNR per receive antenna. The analysis in this section is general and could also be extended to other antenna configurations although we will only use N_t and N_r equal to 2 from now on. Therefore, the CDF of the Eqn. (4) is denoted as

$$F_{SDM} = 1 - \frac{2}{\gamma_0}e^{-\frac{2\gamma_s}{\gamma_0}} \quad . \tag{5}$$

Under the assumption that the per frequency chunk fading statistics is equivalent to flat-rayleigh fading, the CDF of the per stream SINR of the spatial multiplexing scheme is the same as Eqn. (5). This is shown in Fig. 3, curve (1). It is based on a *zero-forcing* (ZF) receiver and assumes that the Geometry factor (G-factor) [2] is equal to 20 dB. For simplicity we assume that all users to have the same G-factor. The reason is that for SDM-FDPS, the users in lower G-factor will use single-stream MIMO schemes instead, which makes the analysis quite complicated. A high value of the G-factor was selected for illustration here since dual stream operation presupposes good channel conditions. The problem with the analysis of spatial multiplexing schemes lies in the fact that different spatial streams with different SINR can support different data rate. To solve this problem, we propose the concept of **unified SINR** for spatial multiplexing MIMO defined as the equivalent single SINR that offers the same instantaneous capacity. As shown in [24], for spatial multiplexing schemes with ZF receiver, the end-to-end system is decoupled into a set of parallel uncorrelated SISO channels (streams). If we assume SINR on the stream i is γ_i, and there is $\mathrm{N_{str}}$ total streams, the unified SINR γ_u can be formulated as:

$$\begin{aligned} \log_2(1+\gamma_u) &= \sum_{i=1}^{\mathrm{N_{str}}} \log_2(1+\gamma_i) \\ \Leftrightarrow \gamma_u &= -1 + \prod_{i=1}^{\mathrm{N_{str}}} (1+\gamma_i) \quad . \end{aligned} \tag{6}$$

[2]The G-factor is the ratio of the total received wideband BS power and othercell/noise interference at the UE. It is averaged over short-term fading, but not shadowing.

If the streams are uncorrelated, and if the signals including interference are furthermore Gaussian, we have independent streams. Following the results on functions of random variables in Chapter 6 of [26], we have

$$\begin{aligned} & F(\gamma_u \leq U) \\ & = \int_1^{U+1} p_{x_1}(x_1) \int_1^{\frac{U+1}{x_1}} p_{x_2}(x_2) \ldots dx_1 \ldots dx_K \\ & = \int_1^{U+1} p_{\gamma_1}(x_1 - 1) \int_1^{\frac{U+1}{x_1}} p_{\gamma_2}(x_2 - 1) \ldots dx_1 \ldots dx_K \quad , \end{aligned} \tag{7}$$

where the $p_{\gamma_i}(\gamma_i)$ is the PDF of γ_i, the $p_{x_i}(x_i)$ is the PDF of $x_i = \gamma_i + 1$. The second line follows because of the PDF relation of a linear function. In the general case, Eqn. (7) is a $\mathrm{N_{str}}$ dimensional integral. For the case of only a few streams Eqn. (7) can be used for closed-form evaluations, whereas Monte Carlo integration is more practical for a higher number of streams.

By inserting the spatial multiplexing stream SINR distribution (Eqn. (4)) into the Eqn. (7) for both $p_{\gamma_1}(\gamma_1)$ and $p_{\gamma_2}(\gamma_2)$, the distribution of unified effective SINR for SU-MIMO can be derived as

$$\begin{aligned} & F_{SU-MIMO}(\gamma_u \leq U) = \\ & \int_1^{U+1} \frac{1}{m} e^{-\frac{x_1 - 1}{m}} (1 - e^{-\frac{\frac{U+1}{x_1} - 1}{m}}) dx_1 \quad , \end{aligned} \tag{8}$$

where $m = \frac{\gamma_0}{2}$. The CDF of Eqn. (8) is shown in Fig. 3, curve (2). Applying the PF criterion, i.e., by adding the multiuser diversity on top, the CDF of the post scheduling per PRB unified SINR for SU-MIMO can be given as

$$F_{SU-MIMO\_K} = (F_{SU-MIMO})^K \quad , \tag{9}$$

The CDF curve given by Eqn. (9) for user diversity order equal to 10 is shown in Fig. 3, curve (3).

In case of MU-MIMO, since the multi-user diversity can be exploited even in the spatial dimension, the multiuser diversity should be utilized before translating into the unified SINR. Therefore, the CDF of the post-scheduling SINR on each stream with multiuser diversity of K is given by

$$F_{SDM\_K} = (F_{SDM})^K \quad , \tag{10}$$

This is shown for user diversity order of 10 in Fig. 3, curve (4). Then the two stream SINRs with the same distribution as in Eqn. (10) are combined into a single effective unified SINR using Eqn. (7), as given by

$$\begin{aligned} & F_{MU\_MIMO\_K}(\gamma_u \leq U) = \\ & \int_1^{U+1} K(1 - e^{-\frac{x_1 - 1}{m}})^{K-1} \frac{1}{m} e^{-\frac{x_1 - 1}{m}} (1 - e^{-\frac{\frac{U+1}{x_1} - 1}{m}})^K dx_1 \quad . \end{aligned} \tag{11}$$

To enable a simple and realistic way of user multiplexing for MU-MIMO, we assume equal power allocation for all users. Therefore, the SINR for certain user will not change even if partner user is different. The post-scheduling per frequency chunk unified SINR distribution for the MU-MIMO case (Eqn. (11)) is shown with 10 users in Fig. 3, curve (5). Comparing the curve (4) and curve (5) in Fig. 3, the unified SINR of the MU-MIMO scheme has a mean SINR gain over that of the SU-MIMO scheme with the same user diversity order due to the extra flexibility in the spatial domain, although the diversity order is approximately the same.

B. Throughput Analysis

Based on the post-scheduling SINR analysis, we are ready to get the performance bounds for each SDM-FDPS cases. One important prerequisite is the choice of the SINR to throughput mapping metric. The most common metric is the Shannon Formula [27] given as:

$$C = \log_2(1 + SNR) \quad . \tag{12}$$

As shown in [17], a better approximation to realistic link adaptation model with realistic MCS is the "***Scaled Shannon***" formula, as proposed in [17]. It is given by

$$C = BW_{eff} \times \log_2(1 + SNR/SNR_{eff}) \quad . \tag{13}$$

Here the BW_{eff} is adjusted according to the system bandwidth (BW) efficiency of the system and SNR_{eff} is adjusted according to the SNR implementation efficiency. The BW_{eff} is 0.83 considering LTE system parameters and SNR_{eff} is 1.6dB in AWGN channel with realistic modulation and coding [17]. Furthermore we upper limit C according to the hard spectral efficiency given by the MCS supported in simulation study, e.g. 64QAM, Rate 4/5.

The throughput at a certain G-factor TP_G is given as

$$TP_G = \int_0^\infty F_{Map}(x) \cdot p_\gamma(x) \cdot dx \quad , \tag{14}$$

where the F_{Map} is the SINR to throughput mapping function which can use either Shannon formula (Eqn. (12)) or Scaled Shannon (Eqn. (13)). The $p_\gamma(x)$ is the PDF of post-scheduling SINR distribution, which can be obtained by taking the derivative of Eqn. (9) for SU-MIMO or Eqn. (11) for MU-MIMO.

With the knowledge of TP_G for each G-factor and the PDF of the G-factor distribution p_G for a certain cellular deployment scenario [28], the cell level throughput can be written as:

$$TP_{cell} = \int_0^\infty TP_G(G) \cdot p_G(G) \cdot dG \quad , \tag{15}$$

where the TP_G is a function of G. Note that the simplified analysis above will only be used to obtain the theoretical bounds, while the detailed system simulation based evaluation in section IV is not limited by these simplifications.

IV. System Level Simulations Based Evaluation

Although the simplified theoretical analysis is very useful in getting insight into the SDM-FDPS performance, it is difficult to include the effect of system imperfections due to the mathematical intractability. Therefore, the SDM-FPDS performance is further evaluated using a system-level simulator. We first propose the practical SDM MIMO aware FDPS algorithms design with practical constraints in subsection IV-A. Following that, subsection IV-B introduces the simulation methodology and default assumptions and the subsection IV-C summarizes and analyzes the simulation results.

A. Proposed Practical MIMO aware FDPS Algorithms

The legacy FDPS algorithm will be extended to the spatial dimension in order to operate with SDM and the MIMO mode selection. In terms of the flexibility of MCS and MIMO adaptation per PRB, although it is still an open issue in 3GPP, full flexibility is hard to achieve due to the signaling constraints. Thus, only one MIMO mode per UE and one MCS per spatial stream are supported within a TTI in this study, which makes the performance suboptimum. However, the algorithm design is efficient and suitable for practical implementation. Moreover, since SDM only makes sense for time-frequency resources experiencing favorable channel conditions, we select transmit diversity schemes as the fallback MIMO mode. In order to support FDPS with full flexibility, we further assume that CQIs for both *single-stream* (SS) and *dual-stream* (DS) MIMO are reported from the UE to the eNode-B. The CQI is reported per

stream for DS MIMO. Based on these considerations we propose the following simple heuristic algorithm which offers a good trade-off between performance and complexity.

In both SU- and MU- MIMO, the first step is to estimate the user throughput using a SNR to supportable throughput mapping table based on the CQIs reported for the individual PRBs for each user. Afterwards the PF metric is calculated for all MIMO cases. For single-stream MIMO and SU-MIMO, we denote PF_SS$_{k,b}(t)$, PF_SU$_{k,b}(t)$ as the PF metric value respectively for each user k within each frequency chunk b at time interval t. And for MU-MIMO, PF_MU$_{k,b,s}(t)$ denotes the corresponding PF metric value. Next, for each frequency chunk b, the best user (or best users for MU-MIMO) is chosen to maximize the PF metric over all available MIMO schemes denoted as PF_SS$_b(t)$, PF_SU$_b(t)$ and PF_MU$_b(t)$ respectively. Note that special care should be taken when precoding is performed with MU-MIMO. The restriction is that the scheduler can only multiplex users with the same preferred precoding matrix, but with orthogonal precoding vectors (i.e., occupy different stream on the same time-frequency resource). The effect of this will be further explained in Section IV-C1. On the basis of the above algorithm, a first round MIMO mode selection is made for each frequency chunk, and user selection is done implicitly as well, as shown in the first block of the flow-charts for the proposed FDPS algorithms for SU- and MU- MIMO in Fig. 4 (a) and (b) respectively.

A potential problem is that multiple MIMO modes can be selected for a single user, i.e., both dual-stream and single-stream mode are selected for the same user on different PRBs, within one TTI, which is a contradiction of the constraint imposed. To avoid an iterative optimization process, the following simple approach is proposed for the two cases. As shown in Fig. 4 (a) for SU-MIMO, whenever there is a conflict, we compare the total throughput from all the single stream PRBs for this user (TP_total_SS) with that from all the dual-stream PRBs (TP_total_DS). Then the user is forced to use the MIMO mode which gives better total throughput. For the MU-MIMO case as shown in Fig. 4 (b), when the single-stream mode is favored for a user, we make a decision for each dual-stream PRB depending on whether the other stream on the same frequency chunk is selected for this user or not. If the user is selected on both streams, this user is forced to single-stream for this frequency chunk, whereas this stream is assigned to the partner user on the same frequency chunk if the opposite is true. Once the assignment of PRBs to users has been performed, the scheduler instructs the LA to calculate the supported data rate for each user, also taking the selected MIMO mode into account.

B. Simulation Methodology and Assumptions

1) Decoupled link and network level simulation methodology: We consider a decoupled link and system-level simulation methodology in this study. This technique is a practical trade-off between simulation inaccuracy due to the modeling simplifications and the processing load caused by the complexity of the joint modeling of link and system levels in realtime [29]. This approach relies on abstraction of the link-level processing in the form of pre-generated SINR traces obtained from a link level simulation tool, while the system-level related processing is implemented in a network overlay. The link level simulator used in this study is described in [30].

2) Network Simulator Modeling: The network simulator provides traffic modeling, multiuser scheduling, and link adaptation including Chase Combining HARQ, based on the UTRAN LTE downlink parameters and assumptions described in [6]. The system is based on a simple *admission control* (AC) strategy which keeps the number of UEs per cell constant. UEs within the reference cell are simulated in detail, while other-cell interference, path loss, and shadowing is modeled as AWGN adjusted to an equivalent G-factor distribution [28]. The average G-factor remains constant for a UE during a session, thus assuming that the packet call is short compared to the coherence time of the shadow fading and distance dependent path loss. Besides, due to the signalling constraints, we assume equal power allocation over the PRBs, and the same MCS is used for all PRBs on each spatial stream for per UE in each TTI. The overhead due to reference symbols and control information is assumed to be equal to two OFDM symbols per TTI (28% overhead). Main system parameters are given in Table I. The modeling details of

modules such as link-to-system mapping, Link Adaptation, CQI, HARQ, and traffic models are further introduced hereafter.

TABLE I
DEFAULT SIMULATION PARAMETERS AND ASSUMPTIONS.

Parameter	**Setting**
Physical parameters	See [1]
System bandwidth	10 MHz
Cell-level user distribution	Uniform
PRB width	375 kHz
User diversity order (UDO)	10 (default)
Packet Size for Finite Buffer Model	Single 2 Mbit
Power delay profile	Typical Urban
LA delay	2 ms
CQI error std	1 dB
CQI reporting resolution	1 dB
Modulation/code rate settings	QPSK: 1/3, 1/2, 2/3 16QAM: 1/2, 2/3, 4/5 64QAM: 1/2, 2/3, 4/5
H-ARQ model	Ideal chase comb.
LA target	20% BLEP (1st TX.)
UE speed	3 km/h
Channel estimation	Ideal
Carrier frequency	2 GHz
autoregressive moving window	150 TTIs
Initial T_k value	log2(1+G/2.5)/UDO
Weight info feedback delay	2 ms

3) Link to System Mapping: For complexity reasons, a link level simulation of all the links between eNode-B and UEs is not feasible. In practice, we utilize the decoupled link and network simulation approach and use single link level simulation results in the form of the BLER as a function of SINR to predict each UE's throughput. The link-to-system mapping table adopted here is based on the Exponential Effective SIR Mapping (EESM) [31] [32]. The motivation behind such a model is to avoid the generation of all BLER curvers for any geometry and channel conditions in the OFDM system. Derivation of EESM is based on the Union-Chernoff bound for error probabilities. The basic idea is to map the current geometry and channel conditions (which will involve frequency selective fading for a multi-path channel) to an effective SIR value that may then be used directly with the AWGN BLER curves to determine the appropriate block error rate. The effective SINR is defined as

$$\text{SINR}_{eff} = -\beta \cdot \ln\left(\frac{1}{N_u}\sum_{j=1}^{N_u} e^{-\frac{\gamma_j}{\beta}}\right) \quad , \tag{16}$$

where N_u is the number of useful sub-carriers being considered, and γ_j is the SINR for the j^{th} OFDM sub-carrier. The β is a parameter that must be estimated from extensive link-level simulations for every MCS being considered, and it could be taken as a parameter to describe the sensitivity of turbo decoder performance towards frequency selectivity. The general trend is that the higher the modulation order and code rate, the worse the decoder performance towards frequency selectivity. The EESM is not only used to predict the throughput from the CQIs in the LA module in transmitter, but also used to calculate the actual throughput from the experienced SINRs per sub-carrier at the receiver.

4) Link Adaptation: With the availability of instantaneous channel conditions, the link adaptation module can adapt its transmission format accordingly and select the MCS that maximizes the spectral efficiency. In this study, the link adaptation consists of both inner loop link adaptation (Adaptive modulation and coding) and outer loop link adaptation.

The procedure for inner link adaptation is as follows. Given one specific MCS i, the corresponding BLER_i can be predicted with the link to system model as explained in Subsection IV-B3. Then the throughput for i^{th} MCS can be predicted as

$$\text{TP}_i = (1 - \text{BLER}_i) \times \text{TBS}_i \quad , \tag{17}$$

where the TBS_i is the transport block size of a certain MCS i. The inner link adaptation chooses the MCS with the best throughput, while maintaining the BLER target for transmission, as given by Eqn. (18).

$$\text{MCS\_SEL} = \arg \max_{i|\text{BLER}_i < \text{BLER}_{\text{target}}} \{\text{TP}_i\} \quad . \tag{18}$$

Further, an outer loop LA (OLLA) module is used to maintain the 1st transmission target BLER by adding an adaptive offset to the available CQI reports for the UE, based on the ACK/NACKs [33] [9]. The OLLA is shown to be very effective in combating the LA error due to imperfect CQI [9].

5) CQI Error and Delay Modelling: To support the LA, the transmitter should have knowledge of the channel variation for each UE. In the FDD system, this information is obtained by CQI feedback from each UE to the eNode-B via uplink. The quality of CQI is an important factor for the efficient application of LA. In our work, the CQI is simply the linearly averaged SINR over the PRB. To take into account the practical imperfections, the CQI reports are modeled with errors associated to (i) measurement inaccuracy modeled as a lognormal error in the SINR domain and a quantization loss with 1dB resolution (ii) reporting delay corresponding to 2 ms.

6) Layer One HARQ Retransmission Model: In this network simulator, explicit scheduling of multiple HARQ processes per user has not been performed due to the associated complexity. Instead we include the effect of HARQ in terms of Chase Combining using a simple HARQ process model from [34]. The soft combined SINR after each transmission is given by:

$$\{\text{SINR}\}_n = \eta^{n-1} \cdot \sum_{k=1}^{n} (\text{SINR})_k \quad , \tag{19}$$

where $\{\text{SINR}\}_n$ represents the combined SINR after n transmissions, η denotes the chase combining efficiency and $(\text{SINR})_k$ denotes the SINR of the k^{th} transmission. $\eta = 0.95$ is assumed in this study, which is the recommended value in [34]. Note that Eqn. (19) is only valid when n is relatively small, e.g., around 3-4, which is also practical. In this study the HARQ process allows a maximum of three retransmissions per block before it is discarded, i.e., $n = 4$. Moreover, we use the simple statistical recursive HARQ model given below to calculate the effective block throughput after retransmissions:

$$\text{TP}_{\text{eff}} = \sum_{k=1}^{n} \frac{\text{TBS}}{k} (1 - \text{BLER}_k) \quad , \tag{20}$$

where TP_{eff} denotes the effective throughput after HARQ combining gain, and TBS denotes the transport block size given by the MCS employed, BLER_k denotes the BLER for the k^{th} transmission. Note that Eqn. (20) is applicable only if the block is finally correctly received after the fourth transmission, i.e., $\text{BLER}_4 = 0$, otherwise the block is considered to be lost.Further, it is assumed that the HARQ ACK/NACKs are received instantaneously and error free.

7) Traffic Modeling: We have considered the *infinite buffer* and the *finite buffer* traffic models in this study to abstract the behavior of best effort traffic. Infinite buffer is the simplest traffic model for system level evaluation, in which the users always have data packets to transmit. The finite buffer model allows downloading of an equal amount of data by each active user, and when the session is terminated, a new UE is immediately admitted. In both cases user locations within the reference cell are generated on the basis of the G-factor distribution for the simulated deployment scenario [28]. In this study, macro-cell case 1 and micro-cell outdoor to indoor environment are considered.

8) Evaluated MIMO Schemes: Since SDM can only be efficiently utilized by users with a good channel quality and high rank MIMO channel, single-stream MIMO schemes should be used as the fallback mode for the users near the cell edge or with low rank MIMO channel conditions. In this study, the schemes are divided into precoding cases and without precoding cases. For no precoding case, we use *per-antenna rate control* (PARC) [35] with *space frequency coding* (SFC) as the fallback mode. The SFC considered here is Alamouti Space Time Coding applied on neighbouring sub-carriers instead of adjacent time symbols. In the unitary precoding case, the TxAA (CL Mode 1 (CLM1) in WCDMA [36]) is utilized for single stream transmission, and dual stream TxAA (D-TxAA) [37] for dual stream transmission. In both cases, the weight is optimized for a group of sub-carriers within a PRB, and the feedback requirements are 2 bits per PRB [38]. Since the optimal design of codebooks specifically for D-TxAA is still an open issue, the CLM1 codebooks are adopted for D-TxAA as well in this study. For comparison purposes, we consider as reference scheme the 1x2 SIMO with PF FDPS [6]. The MIMO schemes and the receiver types considered are summarized in Table II.

TABLE II
MIMO SCHEMES AND RECEIVER TYPES CONSIDERED.

MIMO mode	No precoding	With precoding	Receiver Type
(SU-) MU- MIMO (Dual-stream)	PARC	D-TxAA	Linear MMSE
Fallback mode (Single-stream)	SFC	CLM1	Maximal Ratio Combining (MRC)

C. Simulation Results

1) Finite Buffer Performance: The average cell throughput is plotted against number of active users for different SDM-FDPS schemes in the macro-cell and micro-cell scenarios. For the macro-cell case shown in Fig. 5 it is observed that both SDM schemes without precoding offer only marginal gain over the 1x2 SIMO case, over the considered range. This is due to limited SINR dynamic range available in macro-cells, e.g., the highest G-factor is limited to 17 dB. However, the gain of SDM schemes increases with precoding cases, e.g., at user diversity order of 10 the gain is around 20% over reference scheme. The gain comes mostly from cell edge users benefiting from the CLTD feature. The drawback of precoding cases is the extra weight feedback requirement. Among the precoding cases MU-MIMO outperforms SU-MIMO especially when the user diversity order is low, due to the increase in degree of spatial freedom available to the scheduler.

As for the micro-cell scenario, the results in Fig. 6 convey a slightly different picture. If we take user diversity order of 10 as an example, the SU-MIMO scheme without precoding gives a gain of around 10% over the reference case. When precoding is introduced, the gain from SU-MIMO increases to around 15%. With increasing user diversity order the cell throughput increases very slowly. The behavior of MU-MIMO without precoding is quite different as the cell throughput has a steeper increase than the SU-MIMO curves. Although it is worse than SU-MIMO with precoding when the user diversity order is low, it outperforms SU-MIMO with precoding when user diversity order exceeds 21.

Compared to that of MU-MIMO without precoding, the results of MU-MIMO with precoding grow much slower with the increase in the user diversity order. One of limitations comes from the reduced effective user diversity order due to precoding restriction. As mentioned earlier, for MU-MIMO with precoding, we can only multiplex users with the same preferred precoding matrix, but with orthogonal precoding vectors. For the precoding schemes we considered, namely D-TxAA with 4 precoding quantization matrix options, the active users are divided into 4 groups. Then the effective user diversity order is the number of users with same preferred precoding matrix selection. To further explain this, the probability of distribution of the effective user diversity order traces collected from simulation of MU-MIMO with

precoding is shown for user diversity order of 4, 10, 30 in Fig. 7. As shown, when user diversity order is 4, the effective user diversity order is around 1.8 in average. The average effective user diversity order is only around 3.4 and 8.9 for a user diversity order of 10 and 30. This also suggests a dilemma we might face when MU-MIMO with unitary precoding is used. If we increase the quantization resolution in the precoding matrix, we can improve the link performance since the spatial streams will be made more orthogonal to each other. On the other hand, the effective user diversity order will be reduced, and the gain from FDPS will be lower with less multi-user diversity.

Another limiting factor for the results of MU-MIMO comes from the limited modulation order. As shown in Fig. 8, we plot the CDF of the post-scheduling effective SINR from simulation for selected cases of MU-MIMO with or without precoding. The highest MCS we have used is the 64QAM and 4/5, and for this MCS an effective SINR of 17dB will always have a BLER of 0, that is, the throughput with effective SINR higher than 17dB will saturate. At the user diversity order of 30, the MU-MIMO without precoding has 15% of the time entered the saturation range, while the MU-MIMO with precoding has been in the saturation range around 24% of the time. In summary, when the user diversity order is 10, the gain of MU-MIMO scheme over reference is in the order of 16%-30% depending on whether precoding is used. When the user diversity order is around 48, the gain is in the order of 35%. Results confirm that the SDM concepts are mainly features for the micro-cell scenario.

2) Performance of Finite Buffer versus Infinite Buffer: The traffic model has a significant impact on SDM performance. The average cell gain over 1x2 MRC case with FDPS is plotted for different traffic models in Fig. 9. As shown with finite buffer, the gain is from 10%-30%, and for infinite buffer, the gain is in the order of 50%-60%. Since equal amount of data is sent to all users in the cell, the finite buffer model results in a longer session time for the low data rate cell edge users than the users in good condition. On the other hand, for the infinite buffer model all users will be given equal access time, and the users supporting high data rate can download much more data than users in the cell edge, thus the average cell throughput is increased.

V. Comparison of Theoretical Bounds with Simulation Results

The derived theoretical bounds in section III and the system-level simulation results in section IV are compared here to illustrate the effect from practical factors which is not feasible to be included in theoretical analysis.

The user throughput with SDM-FDPS against G-factor curves are first plotted for the theoretical bounds (using Eqn. (14)) and simulation results in Fig. 10. As observed, a quite good approximations can be found with the scaled Shannon bounds by including realistic LA effect. The remaining difference between the theoretical bounds with the simulation results can be due to some imperfection factors such as the frequency selectivity within a frequency chunk, non-ideal CQI as well as signalling constraints. In some cases quite big difference is observed between bounds and simulation, this is mainly because of the high sensitivity of imperfections in the low G-factor range. On the other hand, compared to the simulations, the relative performance gap of SU-MIMO and MU-MIMO can be modelled quite accurately by the bounds.

Further, we compare the cell level throughput for theoretical approaches (using Eqn. (15)) and simulation results for different cell scenarios, as shown in Fig. 11. The approach using scaled Shannon can make the bound quite close to the Monte Carlo simulations results, i.e., within a 10%-30% range.

VI. Conclusion

In this paper we have examined the performance of the Spatial Division Multiplexing (SDM) MIMO technology together with Frequency Domain Packet Scheduling (FDPS) from both a theoretical as well as system level simulation standpoint. The theoretical performance bounds have been obtained by deriving the post-scheduling SINR distribution for SDM-FDPS with a simplified analytical model of the Proportional Fair (PF) scheduler. In addition, more realistic link adaptation model have been considered to calculate the performance bounds. The second part of the study utilizes the system level simulator to obtain the

achievable performance including the impact of many other gain mechanisms in the system as well as system imperfections. Firstly, considering practical system design, we proposed the SDM-FDPS algorithms with many practical constraints in mind. Based on UTRAN LTE downlink framework, results reveal the impact on attainable performance from traffic model, precoding, signalling constraints and confirms that SDM-FDPS is a very promising technique for micro-cell type of cellular deployment scenario. Finally, the theoretical bounds are shown to be able to predict the realistic system simulation results within a 10%-30% range. The signalling overhead to support SDM-FDPS is further addressed in [39] where quite significant signalling overhead can be reduced with a relatively small loss. Furthermore, although LTE is chosen as the case study here, the SDM-FDPS anlaysis is generally applicable for many MIMO-OFDM systems, such as WiMAX [5].

REFERENCES

[1] T. E. Kolding, "Link and system performance aspects of proportional fair scheduling in WCDMA/HSDPA," in *IEEE 58th Vehicular Technology Conference*, Orlando, USA, October 2003.

[2] DMB, "The world DMB forum," http://www.worlddab.org.

[3] DVB, "The global standard for digital television," http://www.dvb.org.

[4] IEEE, "Part 11: Wireless LAN medium access control (MAC) and physical layer (PHY) specifications: High-speed physical layer in the 5 ghz band," IEEE 802.11a, Technical Specifications, 1999.

[5] ——, "Local and metropolitan area networks: Part 16, air interface for fixed broadband wireless access systems," IEEE 802.16a, Technical Specifications, 2001.

[6] 3GPP, "Physical Layer Aspects for Evolved UTRA," Technical Specification Group Radio Access Network, Technical Specification TR 25.814 (V 7.1.0), Oct. 2006.

[7] J. H. Sung and J. R. Barry, "Bit-allocation strategies for MIMO fading channels with channel knowledge at transmitter," in *IEEE 57th Vehicular Technology Conference*, vol. 2, Apr. 2003, pp. 813– 817.

[8] W. Rhee and J. M. Cioffi, "Increase in capacity of multiuser OFDM system using dynamic subchannel allocation," in *The 51th IEEE Vehicular Technology Conference*, vol. 2, May 2000, pp. 1085–1089.

[9] A. Pokhariyal, T. E. Kolding, and P. E. Mogensen, "Performance of downlink frequency domain packet scheduling for the UTRAN Long Term Evolution," in *The 17th IEEE Personal, Indoor and Mobile Radio Communications*, Sep. 2006, pp. 1–5.

[10] S. Vishwanath, N. Jindal, and A. Goldsmith, "On the capacity of multiple input multiple output broadcast channels," in *The IEEE International Conference on Communications*, vol. 3, Sep. 2002, pp. 1444–1450.

[11] M. Costa, "Writing on dirty paper," *IEEE Transactions on Information Theory*, vol. 29, pp. 439–441, May 1983.

[12] R. W. Heath Jr., M. Airy, and A. J. Paulraj, "Multiuser diversity for MIMO wireless systems with linear receivers," in *The 35th Asilomar Conference, Signals, Systems, and Computers*, vol. 2, Nov. 2001, pp. 1194–1199.

[13] K. Jung, C. S. Park, and K. B. Lee, "Bit and power allocation for MIMO-OFDM systems with spatial mode selection over frequency-space-time-selective channels," in *The 60th IEEE Vehicular Technology Conference*, vol. 5, Sep. 2004, pp. 3404–3408.

[14] M. Airy, S. S., and R. W. J. Heath, "Spatially greedy scheduling in multi-user mimo systems," in *The Asilomar Conference on Signals, Systems and Computers*, vol. 1, Pacific Grove, Canada, November 2003, pp. 982 – 986.

[15] M. Airy, R. W. J. Heath, and S. S., "Multi-user diversity for the multiple antenna broadcast channel with linear receivers: Asymptotic analysis," in *The Asilomar Conference on Signals, Systems and Computers*, vol. 1, Pacific Grove, Canada, November 2004, pp. 886 – 890.

[16] G. Caire and S. S. Shamai, "On achievable rates in a multi-antenna broadcast downlink," in *The Allerton Conference on Cummunication, Control and Combuting*, Monticello, USA, October 2000, pp. 1188 – 1193.

[17] P. E. Mogensen, N. Wei, A. Pokhariyal, I. Kovacs, F. Frederiksen, K. Pedersen, K. Hugl, T. E. Kolding, and M. Kuusela, "LTE capacity versus Shannon," in *IEEE 65th Vehicular Technology Conference*, Apr. 2007.

[18] A. van Zelst, "Per-antenna-coded schemes for MIMO OFDM," in *IEEE International Conference on Communications*, vol. 4, 2003, pp. 2832–2836.

[19] Freescale Semiconductor Inc., "Aspects of SU/MU Switching and MU-MIMO in DL EUTRA," 3GPP, Sorrento, Italy, TSGR1#47 R1-070222, Feb. 2006.

[20] J. M. Holtzman, "CDMA forward link waterfilling power control," in *IEEE 51st Vehicular Technology Conference*, Tokyo, Japan, May 2000, pp. 1636–1667.

[21] C. Wengerter, J. Ohlhorst, and A. G. E. v. Elbwart, "Fairness and throughput analysis for generalized proportional fair frequency scheduling in ofdma," in *IEEE 61th Vehicular Technology Conference*, May. 2005.

[22] H. Holma and A. Toskala, *WCDMA for UMTS*, revised edition ed. Chichester, UK: Wiley, 2001.

[23] L. T. Berger, T. E. Kolding, J. Ramiro-Moreno, P. Ameigeiras, L. Schumacher, and P. E. Mogensen, "Interaction of transmit diversity and proportional fair scheduling," in *IEEE 57th Vehicular Technology Conference*, Apr. 2003.

[24] J. H. Winters, J. Salz, and R. D. Gitlin, "The impact of antenna diversity on the capacity of wireless communication systems," *IEEE Transactions on Communications*, vol. 42, pp. 1740 – 1751, FEBRUARY/MARCH/APRIL 1994.

[25] D. Gore, R. W. Heath Jr., and A. Paulraj, "On performance of the zero forcing receiver in presence of transmit correlation," in *ISIT*, July 2002, p. 159.

[26] A. Papoulis, *Probability, Random Variables, and Stochastic Processes*, 3rd ed. McGraw-Hill, Inc., 1991.

[27] C. E. Shannon, "A mathematical theory of communications," *Bell Sys. Tech. Journal*, vol. 27, pp. 379–423, 623–656, 1948.

[28] I. Z. Kovács, K. I. Pedersen, J. Wigard, F. Frederiksen, and T. E. Kolding, "Hsdpa performance in mixed outdoor-indoor micro cell scenarios," in *The 17th IEEE Personal, Indoor and Mobile Radio Communications*, Sep. 2006.
[29] L. T. Berger, "Performance of multi-antenna enhanced hsdpa," Dissertation, Aalborg University, April 2005.
[30] N. Wei, A. Pokhariyal, C. Rom, B. E. Priyanto, F. Frederiksen, C. Rosa, T. B. Srensen, T. E. Kolding, and P. E. Mogensen, "Baseline E-UTRA downlink spectral efficiency evaluation," in *The 64th IEEE Vehicular Technology Conference*, Sep. 2006.
[31] Ericsson, "Effective SNR mapping for modelling frame error rates in multiple-state channels," 3GPP2, Tech. Rep. C30-20030429-010, 2003.
[32] ——, "OFDM exponential effective SIR mapping validation," Technical Specification Group Radio Access Network, Tech. Rep. R1-04-0089, 2004.
[33] M. Nakamura, Y. Awad, and S. Vadgama, "Adaptive control of link adaptation for high speed downlink packet access (HSDPA) in W-CDMA," in *The 5th Wireless Personal Multimedia Communications Conference*, vol. 2, Oct. 2002, pp. 382–386.
[34] F. Frederiksen and T. E. Kolding, "Performance and modeling of WCDMA/HSDPA transmission/H-ARQ schemes," in *IEEE 56th Vehicular Technology Conference*, Sep. 2002.
[35] S. T. Chung, A. Lozano, and H. Huang, "Approaching eigenmode BLAST channel capacity using V-BLAST with rate and power feedback," in *The 54th IEEE Vehicular Technology Conference*, vol. 2, Oct. 2001, pp. 915–919.
[36] 3GPP, "Physical layer procedures (FDD) (Release 1999)," Technical Specification Group Radio Access Network, Technical Specification TS 25.214 (V 3.3.0), Jun. 2000.
[37] Motorola, "MIMO evaluation proposal," 3GPP, Denver, USA, TSGR1#44 R1-060615, Feb. 2006.
[38] N. Wei, B. Talha, T. B. Srensen, T. E. Kolding, and P. E. Mogensen, "Spectral efficiency of closed-loop transmit diversity with limited feedback for UTRA Long Term Evolution," in *The 17th IEEE Personal, Indoor and Mobile Radio Communications*, Sep. 2006.
[39] N. Wei, A. Pokhariyal, T. B. Srensen, T. E. Kolding, and P. E. Mogensen, "Mitigating signalling requirement for MIMO with frequency domain packet scheduling," in *IEEE 65th Vehicular Technology Conference*, Apr. 2007.

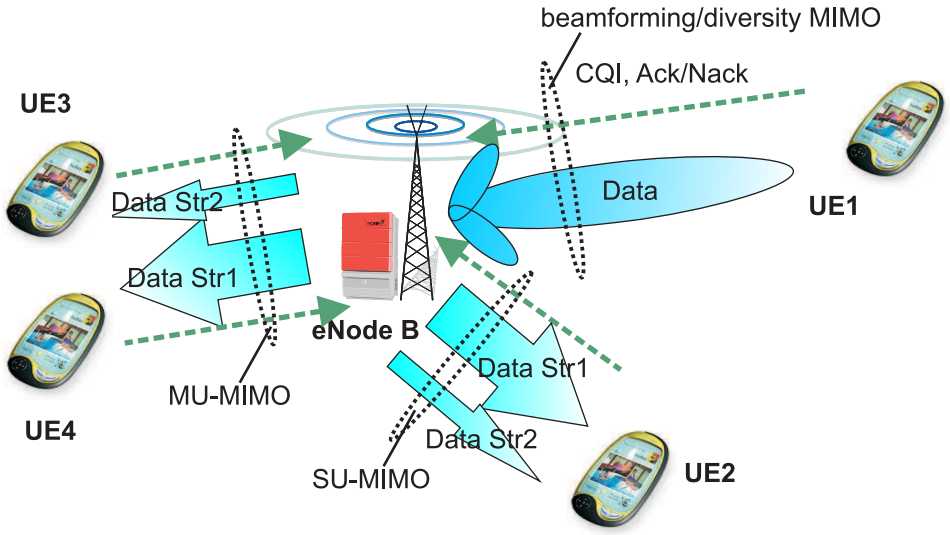

Fig. 1. Illustration of the main principles of UTRA LTE downlink.

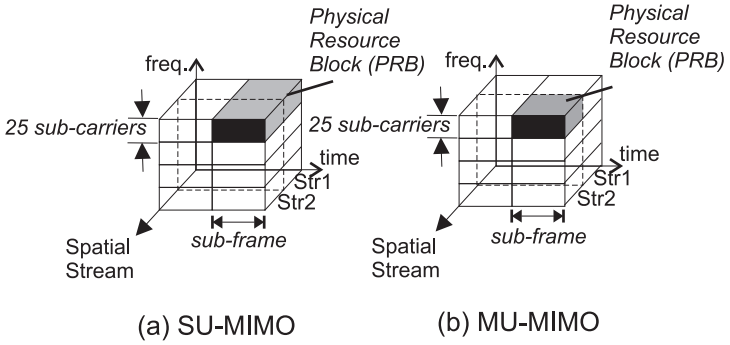

Fig. 2. Illustration of 3GPP LTE SU-MIMO and MU-MIMO concepts.

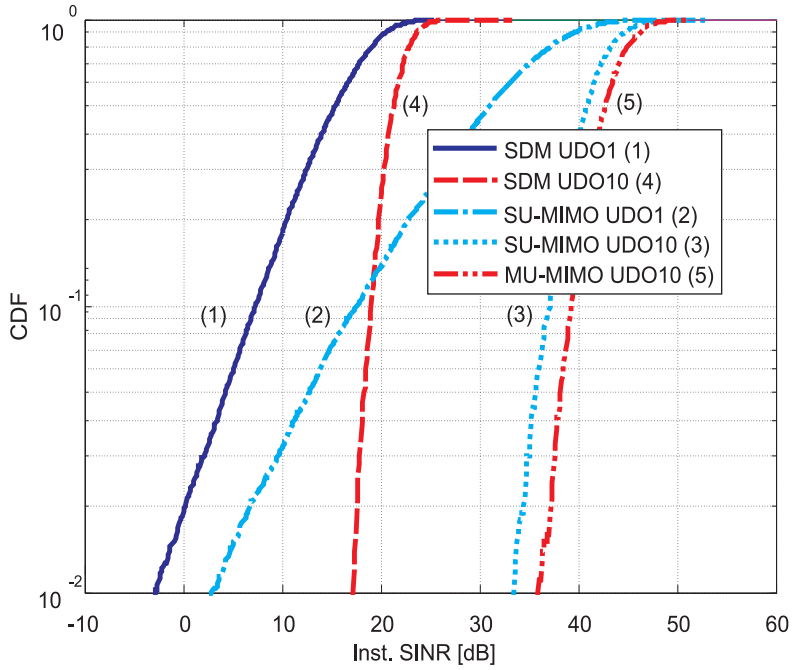

Fig. 3. SINR distributions of the SU-MIMO and MU-MIMO schemes at the G-factor of 20 dB. with and without multi-user diversity order of 10

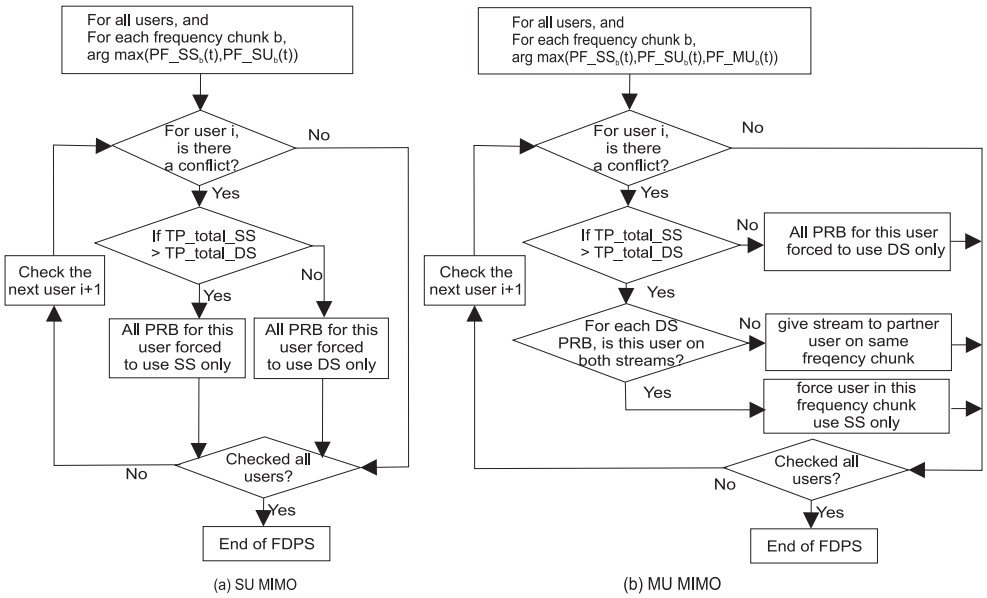

Fig. 4. Flow chart of FDPS algorithm for SU- and MU- MIMO.

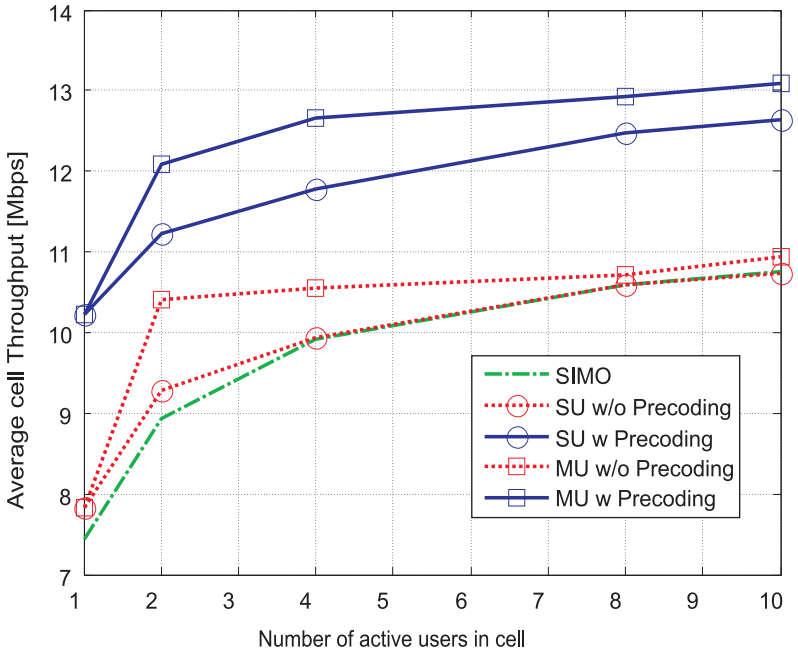

Fig. 5. Average cell throughput comparison of SDM MIMO schemes in macro cell with finite buffer best effort traffic model.

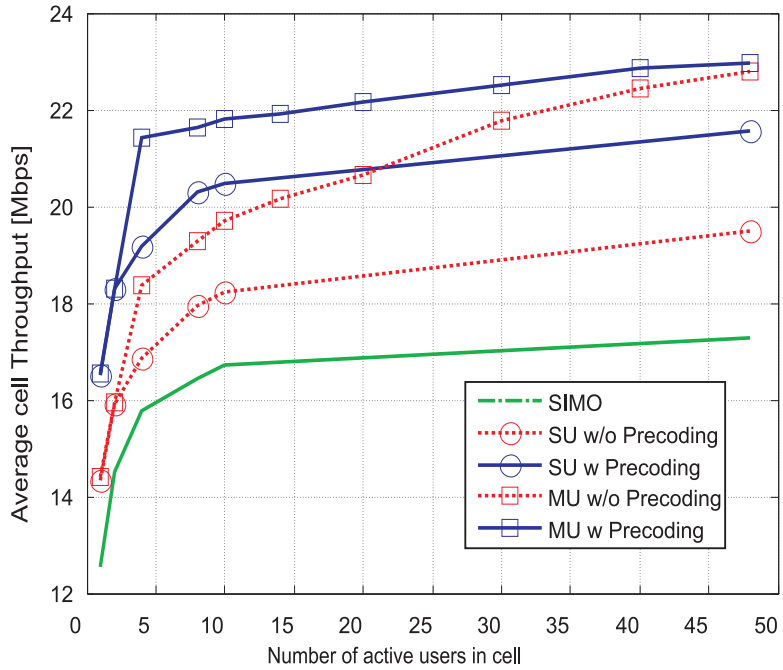

Fig. 6. Average cell throughput comparison of SDM MIMO schemes in micro cell with finite buffer best effort traffic model.

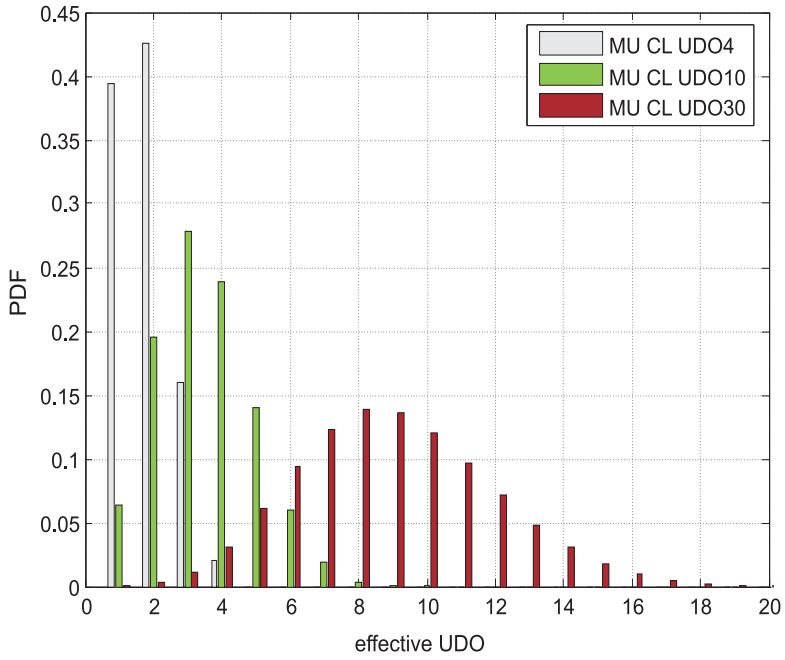

Fig. 7. The sample PDF distribution of the effective user diversity order (UDO) measured from simulation.

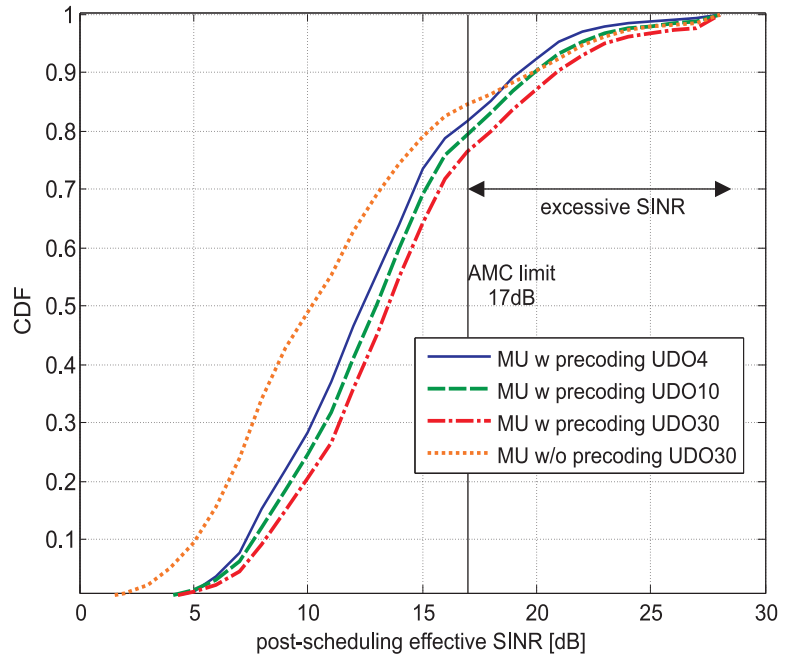

Fig. 8. The sample CDF distribution of post-scheduling effective SINR from simulation.

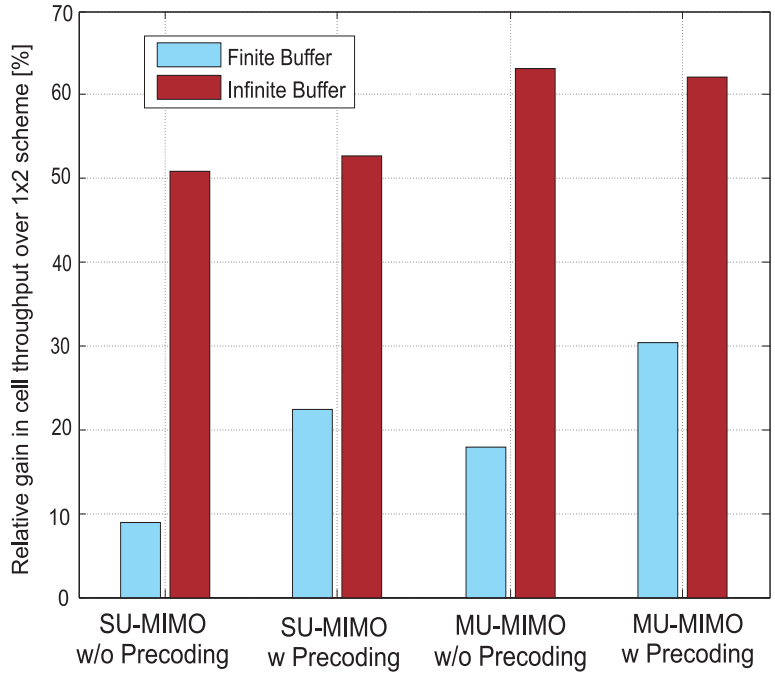

Fig. 9. Relative cell throughput gain of SDM FDPS over 1x2 FDPS in micro cell for different traffic model at user diversity order of 10.

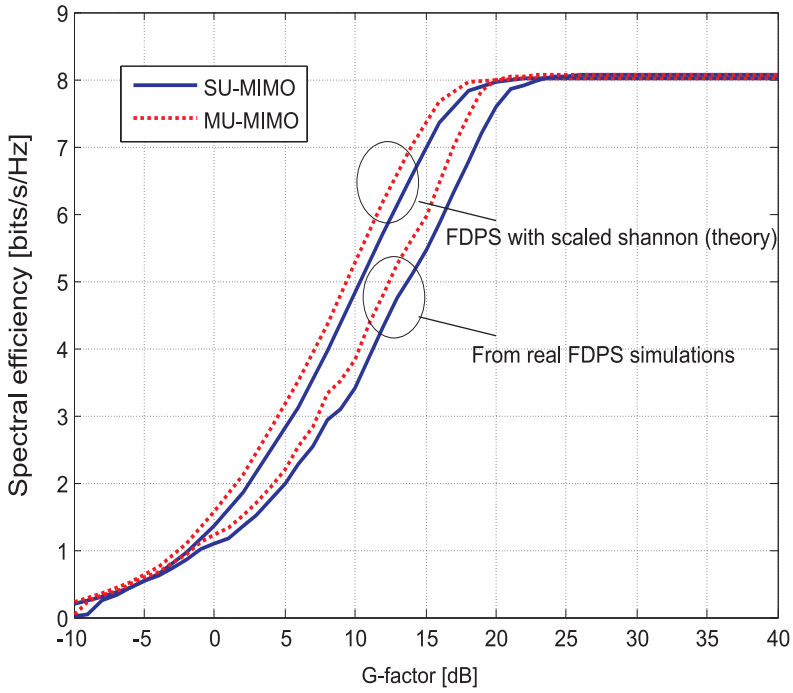

Fig. 10. Comparison of G-factor versus throughput between theoretical bounds and simulation results.

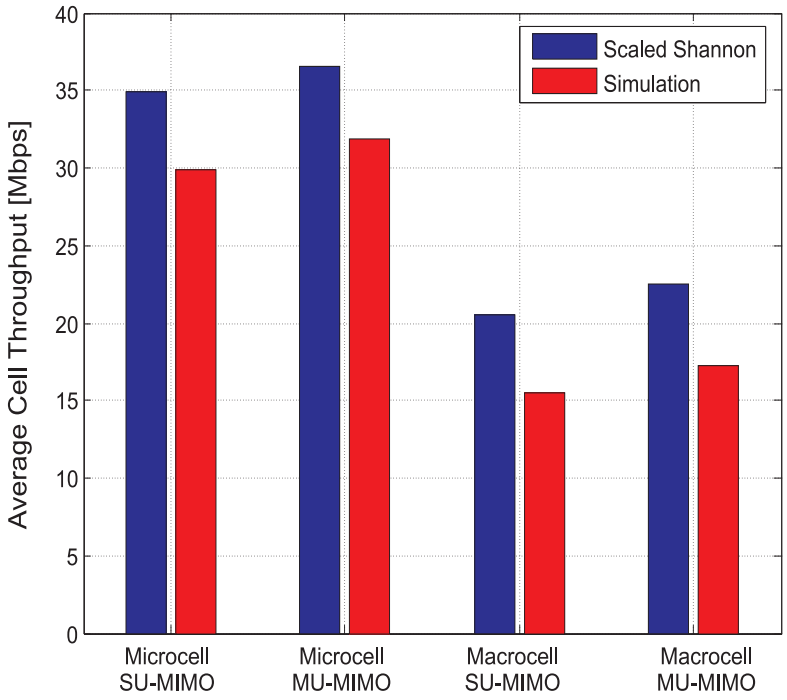

Fig. 11. Comparison of cell throughput between theoretical bounds and simulation results under infinite buffer best effort traffic model.